

## Supplementary Information for

# A Comprehensive Observational Based Multiphase Chemical Model Analysis of the Sulfur Dioxide Oxidations in both Summer and Winter

5

Huan Song<sup>1</sup>, Keding Lu<sup>1\*</sup>, Can Ye<sup>1</sup>, Huabin Dong<sup>1</sup>, Shule Li<sup>1</sup>, Shiyi Chen<sup>1</sup>, Zhijun Wu<sup>1</sup>, Mei Zheng<sup>1</sup>, Limin Zeng<sup>1</sup>, Min Hu<sup>1</sup> & Yuanhang Zhang<sup>1</sup>

<sup>1</sup>State Key Joint Laboratory of Environmental Simulation and Pollution Control, College of Environmental Sciences and Engineering, Peking University, Beijing, China

10 Correspondence to: Keding Lu (k.lu@pku.edu.cn)

### **This PDF file includes:**

Supplementary text

Figures S1 to S9

Tables S1 to S9

15 SI References

## Supplementary Information Text

### Text S1. Activity coefficients of main reactants in the PKU-MARK model

20 The properties of electrolytes play an important role in the kinetic salt effect in the aqueous phase reaction. Atmospheric heterogeneous reactions occurring in aerosol deliquescent particles are characterized by high ionic strength ( $I_s$ ). In these multicomponent mixture, reaction rates should be replaced by the activity coefficient, which representing the thermodynamic non-ideality caused by all-molecular interactions (Rusumdar et al., 2016; Rusumdar et al., 2020). Suitable multiphase chemistry models should apply activity coefficients instead of reaction rate constants in non-ideal solution. Heterogeneous processes in clouds and haze may be considered as occurring in dilute electrolytes and there is no need to consider the influence of ionic strength, this is not the case for high ionic strength deliquescent particles. Based on the measurement of ambient aerosol deliquescent particles (Herrmann et al., 2015), in marine areas, the ionic strength is about 6 M and in urban environments can reach about 8-18 M. Fountoukis and Nenes using the ISORROPIA-II model predicted high levels of ionic strength ranging between 13 and 43 M during the severe Beijing Haze (Fountoukis and Nenes, 2007a). In some extreme cases, the ionic strength of aerosol deliquescent particles can even reach 100 M (Cheng et al., 2016a). In two field campaigns mentioned in this study, the mean value of ionic strength is  $56.55 \pm 39.83$  M ( $\pm 1\sigma$ ) in winter and  $24.26 \pm 13.3$  M ( $\pm 1\sigma$ ) in summer in haze periods ( $PM_{2.5} > 75 \mu\text{g}/\text{m}^3$ ), and in extremely situation, 175.45 M in winter and 96.41 M in summer. In these cases, large errors can be introduced in the model calculation without considering the influence of ionic strength on aqueous phase reaction rate and heterogeneous mass transport.

35 Several studies are developed to evaluate the effects of ionic strength on the activity of aqueous phase ions and organic matters (Pitzer, 1991; Li et al., 1994; Polka et al., 1994; Ming and Russell, 2002; Raatikainen and Laaksonen, 2005; Clegg et al., 2008; Zuend et al., 2008; Zuend et al., 2011), and during the latest year considerable effort has been devoted to developing kinetic model frameworks for the modelling of processes in multicomponent atmospheric particles, which include both a detailed description of organic and inorganic multiphase chemistry as well as detailed thermodynamic comprehensions of its non-ideal behavior (Rusumdar et al., 2016). In this study, the activity coefficients of TMI were calculated by the Extended Debye-Hückel equation (Ross and Noone, 1991; Linder and Murray, 1982; Kontogeorgis et al., 2018). Other ions and organic oxalic acid and its complexes used the typical values predicted by AIOMFAC model by Rusumdar (Rusumdar et al., 2020). As for neutral solutes which activity coefficients are not corrected in AIOMFAC model, such as  $O_3$ ,  $O_2$  and small molecules OH and  $HO_2$ , logarithm of the activity coefficient of neutral solutes is a linear function of the effective ionic strength and the Sechenov coefficient (Rischbieter et al., 2000; Beltran, 2003; Clever, 1983; Ross and Noone, 1991). Unfortunately, Sechenov parameters are unknown for  $H_2O_2$ , which is an important source of aqueous OH radical and other ROS. Several studies (Ali et al., 2014; Cheng et al., 2016b; Liu et al., 2020) showed that the formation rate of S(VI) by  $H_2O_2$  increases with aerosol condensed phase solution ionic strength and proposed different expression with the limitation of maximal ionic strength equal

to 5 M. In this case, considering the high value of ionic strength in the two field campaigns (averaged values are beyond 5 M),  
50 direct extrapolation of the observed/predicted  $a-I$  relationship into such high ranges of ionic strength may not be appropriate.  
Thus, in this paper, the activity coefficient of  $H_2O_2$  is only considered when calculating the sulfate formation rate.  
Corresponding typical activity coefficient values and calculation expressions are summarized in **Table S2 and S3**. The  
influence of ionic strength on gas phase molecular Henry's law coefficients were also considered in the MARK model which  
are summarized in **Table S3**.

55

### **Text S2. The concentration of aerosol particle transition metals in urban areas**

For the lack of Mn concentration in  $PM_{2.5}$  during two field campaigns, we summarized the concentration of transition metals  
in urban areas, mainly in Beijing winter in **Table S9**. The mass concentration ratio of Fe/Mn is in the range of 8.6 to 31 in  
Beijing, and can up to 78 in India. In the calculation of sulfate formation, we used the mass concentration ratio of Fe/Mn as 28  
60 which is a medium value of the ratios. The modeled ratio of soluble Fe (III) to total Fe in the whole winter field campaign was  
in the range of 0.02% to 27.63% with an average value of 1.63% and in the range of 0.04% to 3.29% with an average value of  
0.79% in polluted and highly polluted conditions. The modeled ratio of soluble Mn (II) to total Mn in the whole winter field  
campaign was in the range of 0.01% to 97.21% with an average value of 21.78% and in the range of 0.01% to 80.46% with an  
average value of 19.83% in polluted and highly polluted conditions.

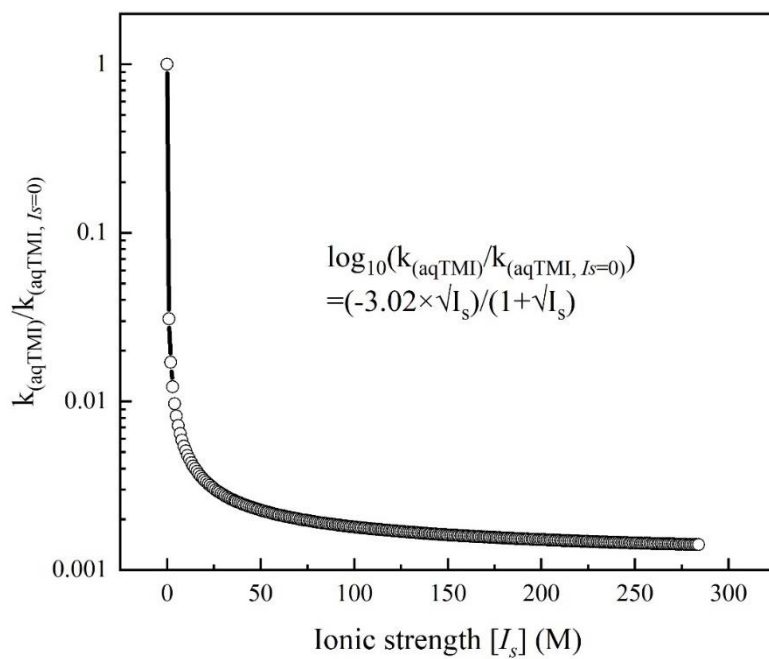
65

### **Text S3. Four haze periods in PKU-17 observation**

Fig. S4 shows the diurnal trends of the key parameters measured in the PKU field campaign for four haze periods. All four  
haze periods lasted for 6 days. Due to the strict emission control policies enacted by the Chinese government, the concentration  
of  $PM_{2.5}$  decreased compared to the same period in 2016 while still cause severe haze pollution in 2017.  $H_2O_2$  exhibited a  
70 typical diurnal pattern with a maximum in the afternoon and low concentrations in the morning and night. It was worth  
mentioning that some studies reported high  $H_2O_2$  concentrations during haze episodes, while in our study the average  
concentration of  $H_2O_2$  was only about 0.02 ppb. Low OH radicals and  $O_3$  concentrations indicated low photochemical activity.  
The largest  $PM_{2.5}$  concentrations of period IV and II were observed exceeding  $150 \mu g/m^3$ , which was coincident with higher  
concentrations of transition metal including Fe and Cu. Period IV was characterized by lower gas-phase  $H_2O_2$  and higher RH  
75 as well as higher aerosol liquid water content compared to the other three periods. Due to the lack of OH radical data during  
Period IV, averaged OH concentrations from the other three haze periods were used in the calculation causing small biases  
due to the reduced gas-phase oxidant pathway during the haze period. Period II was characterized with the highest  $SO_2$   
concentration which was beneficial to the formation of secondary sulfate aerosol. The other two haze periods including Period  
I and Period III also own high levels of 24-hour averaged  $PM_{2.5}$  loading exceeding  $75 \mu g/m^3$ . However, according to the

80 observed  $\text{SO}_4^{2-}$  concentration, high concentrations of sulfate only appeared in the fourth stage of pollution indicating the importance of RH and aerosol TMI.

## Figures



85 Fig. S1. Ionic strength of aerosol particle solution influence on the aqTMI rate constant.

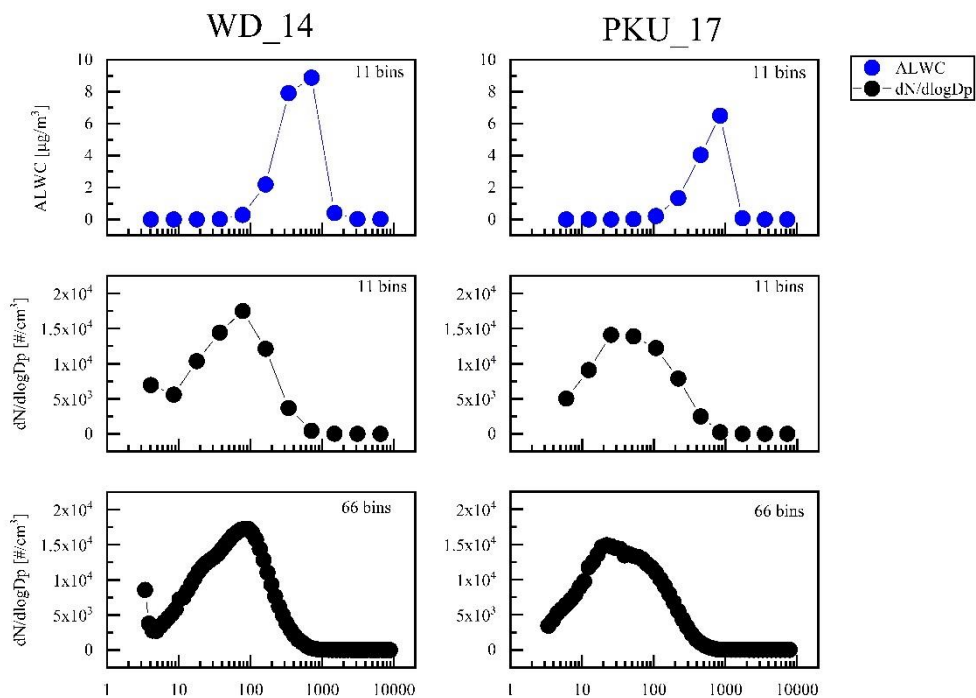


Fig. S2. Distribution of ALWC and number concentration with aerosol particle bins in two campaigns.

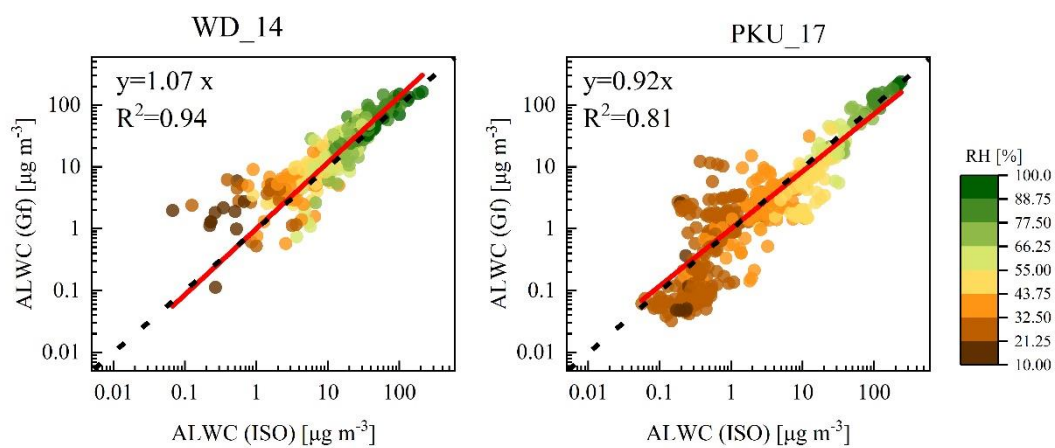


Fig. S3. Calculated aerosol water by ISORROPIA-II model and H-TDMA method in two field campaigns during haze periods. The plots were colored with the relative humidity values. The black dashed line in the figure is the 1:1 baseline, and the red solid line is the linear fitting result assuming the intercept is zero.

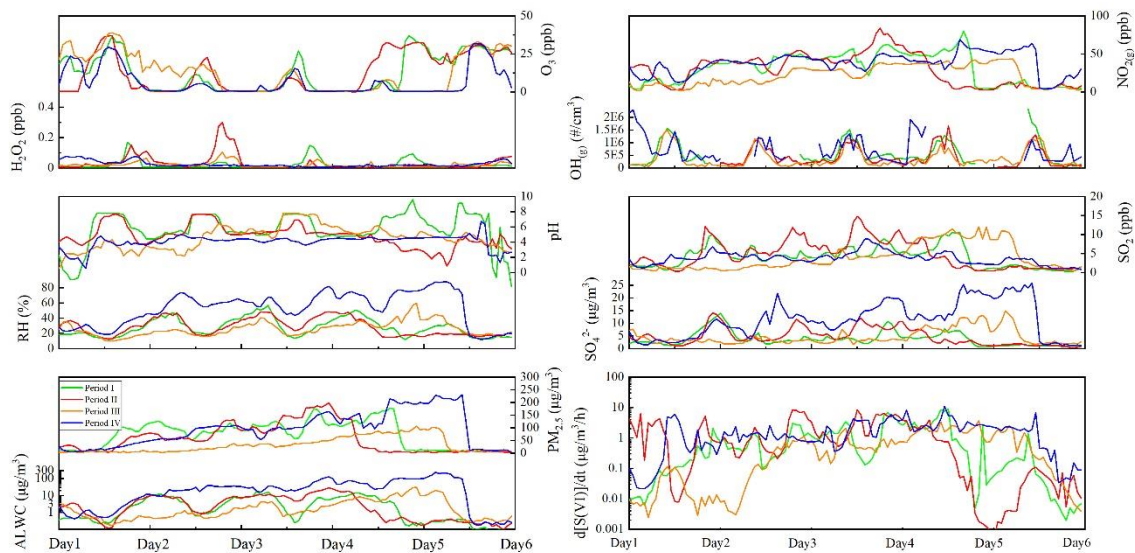


Fig. S4. Time series of observed gas-phase pollutants concentrations, RH, Temperature, PM<sub>2.5</sub> mass loading and calculated aerosol pH and water content and sulfate formation rates in these four haze periods in PKU-17 field campaign.

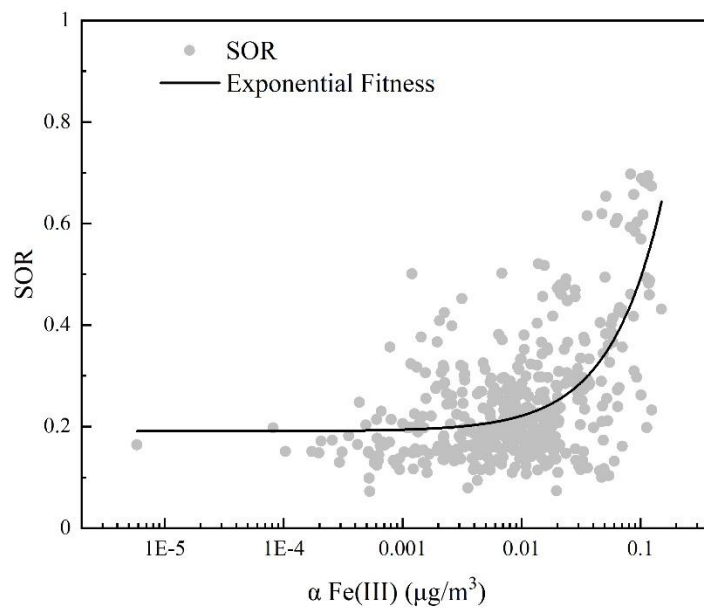
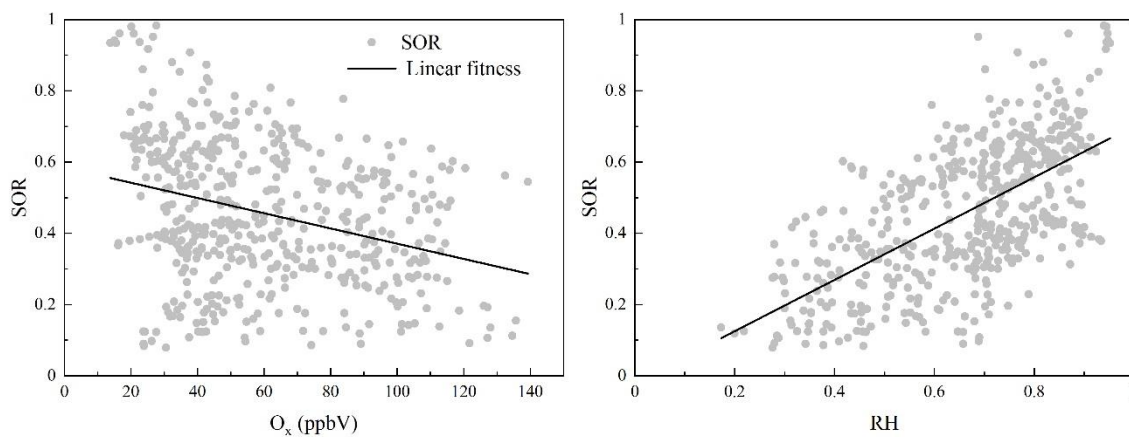


Fig. S5. SOR ( $\equiv n(\text{SO}_2)/n(\text{SO}_2+\text{SO}_4^{2-})$ ) correlations with effective Fe (III) concentrations in PKU-17 winter field campaign.



105 Fig. S6. SOR ( $\equiv n(\text{SO}_2)/n(\text{SO}_2+\text{SO}_4^{2-})$ ) correlations with odd oxygen ( $[\text{O}_x] \equiv [\text{O}_3] + [\text{NO}_2]$ ) and relative humidity (RH) in WD-14 summer field campaign.



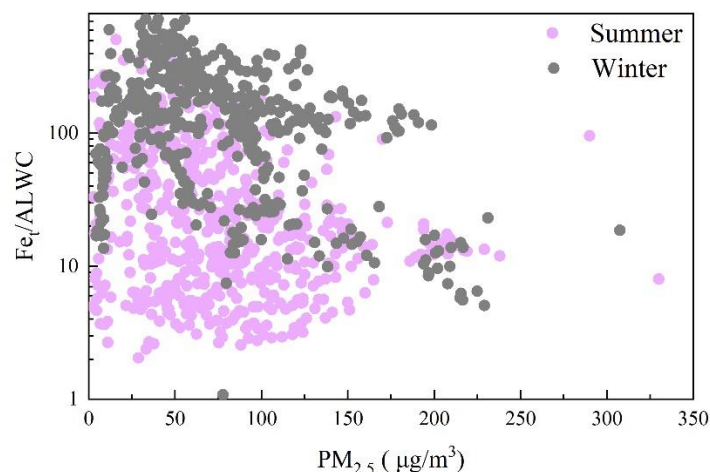


Fig. S7 The “dilution effect” of Fe mass concentration and ALWC increasing with PM mass in winter and summer.

110

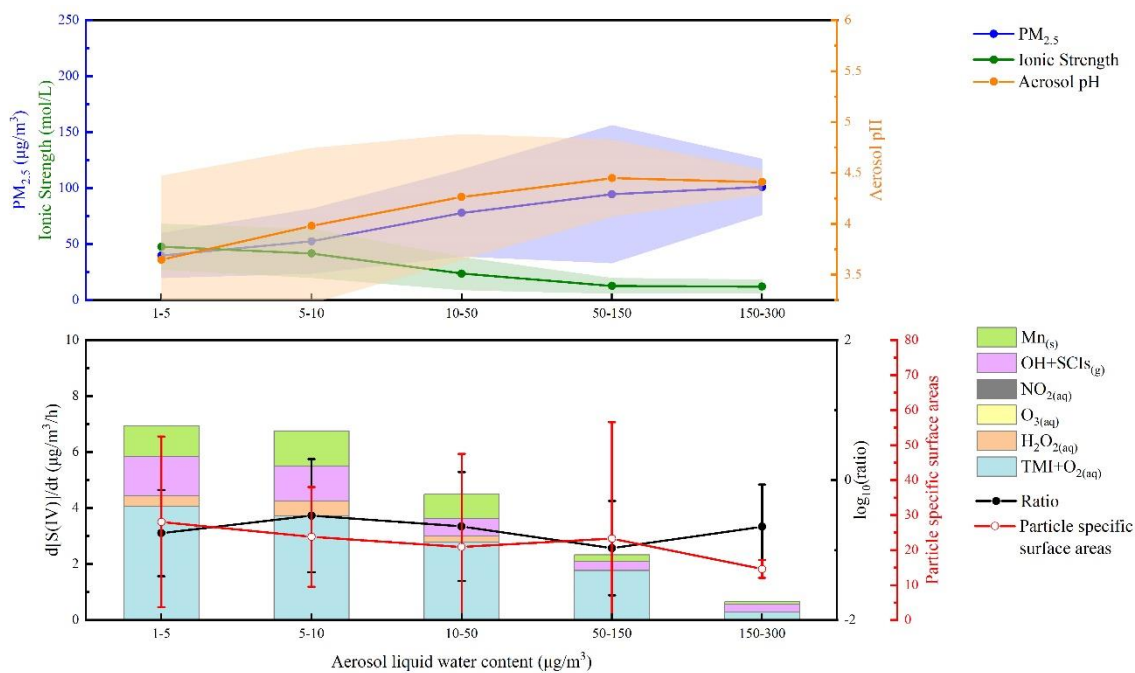


Fig. S8. Variation of PM<sub>2.5</sub>, ionic strength, aerosol pH, particle specific surface areas and sulphate formation rates from different pathways with aerosol liquid water content (ALWC) during summer field campaign. The total number of valid data points shown in the figure is 501. The shaded area refer to the error bar (±1 σ) of PM<sub>2.5</sub> mass concentration, aerosol ionic strength and pH calculated by ISORROPIA-II(Fountoukis and Nenes, 2007b). Ratio in the second panel refers to the ratio of contributions from Mn-surface and aqTMI to produce sulphate. Particle specific surface areas represent the ratio of particle surface area (μm<sup>2</sup>/cm<sup>3</sup>) and mass concentration (μg/m<sup>3</sup>).

115

## Tables

120 Table S1. Reaction rate expression and constant for SO<sub>2</sub> oxidation by OH in the gas-phase.

| Oxidant | The reaction rate expression and constant <sup>a</sup>  | References               |
|---------|---|--------------------------|
| OH      | $R_{\text{SO}_2+\text{OH}} = k_0[\text{SO}_2(\text{g})][\text{OH}(\text{g})]$<br>$k_{0\text{low}} = 3.3 \times 10^{-31} \times (T/300\text{K})^{-4.3} \text{ cm}^6 \text{ s}^{-1}$<br>$k_{0\text{high}} = 1.6 \times 10^{-12} \text{ cm}^3 \text{ s}^{-1}$<br>$F_c = 0.6$ | Burkholder et al. (2020) |

<sup>a</sup> We report the low and the high pressure limit of  $k$  for SO<sub>2</sub> oxidation by OH.  $F_c$  is used to calculate the dependence of  $k$  on pressure and temperature (details see the reference(Burkholder et al., 2020)).

125 Table S2. Aqueous-phase reaction rate expressions, rate constants (k) and influence of ionic strength (Is) on k for sulfate production in aerosol particle condensed phase.

| Oxidants                        | The reaction rate expressions ( $R_{S(IV)+oxi}$ ), constants (k) and influence of $I_s$ (in unit of M) on $k^a$ | Notes                          | References                                     |
|---------------------------------|---|--------------------------------|--|
| O <sub>3</sub>                  | $(k_1[\text{H}_2\text{SO}_3] + k_2[\text{HSO}_3^-] + k_3[\text{SO}_3^{2-}]) [\text{O}_3(\text{aq})]$            |                                | Seinfeld and Pandis (2016)                     |
|                                 | $k_1 = 2.4 \times 10^4 \text{ M}^{-1} \text{ s}^{-1}$   |                                |  |
|                                 | $k_2 = 3.7 \times 10^5 \times e^{(-5530 \times (1/T - 1/298))} \text{ M}^{-1} \text{ s}^{-1}$                   |                                |  |
|                                 | $k_3 = 1.5 \times 10^9 \times e^{(-5280 \times (1/T - 1/298))} \text{ M}^{-1} \text{ s}^{-1}$                   |                                |  |
|                                 | $\log_{10}\left(\frac{k}{k_{I_s=0}}\right) = b_1 \left( \frac{\sqrt{I_s}}{1 + \sqrt{I_s}} - 0.3I_s \right)$     | $I_{s, \max} = 0.94 \text{ M}$ | Maahs (1983)                                   |
|                                 | $b_1$ is in range of 0.7 to 1.3 <sup>b</sup>  |                                |  |
|                                 | $\frac{k}{k_{I_s=0}} = 1 + b_2 I_s$   | $I_{s, \max} = 1.2 \text{ M}$  | Lagrange et al. (1993)                         |
|                                 | $b_2$ is in range of 1.34 to 6.13 <sup>b</sup>  |                                |  |
| H <sub>2</sub> O <sub>2</sub>   | $k_4[\text{H}^+][\text{HSO}_3^-][\text{H}_2\text{O}_2(\text{aq})]/(1 + K[\text{H}^+])$                          |                                | McArdle and Hoffmann (1983)                    |
|                                 | $k_4 = 7.45 \times 10^7 \times e^{(-4430 \times (1/T - 1/298))} \text{ M}^{-1} \text{ s}^{-1}$                  |                                |  |
|                                 | $K = 13 \text{ M}^{-1}$   |                                |  |
|                                 | $\log_{10}\left(\frac{k}{k_{I_s=0}}\right) = 0.36I_s - \frac{1.018\sqrt{I_s}}{1 + 0.17\sqrt{I_s}}$              | $I_{s, \max} = 5 \text{ M}$    | Maaß et al. (1999)                             |
|                                 | $\ln\left(\frac{k}{k_{I_s=0}}\right) = 30.374 - \frac{6824.2068}{215.365 + I_s}^c$                              |                                | Liu et al. (2020)                              |
| NO <sub>2</sub>                 | $k_5[\text{S(IV)}] [\text{NO}_2(\text{aq})]^d$  |                                | Clifton et al. (1988); Lee and Schwartz (1983) |
|                                 | $k_{5\text{low}} = 2 \times 10^6 \text{ M}^{-1} \text{ s}^{-1}$   |                                |  |
|                                 | $k_{5\text{high}} = (1.24 - 2.95) \times 10^7 \text{ M}^{-1} \text{ s}^{-1}$                                    |                                |  |
|                                 | $\log_{10}\left(\frac{k}{k_{I_s=0}}\right) = b_3 I_s$   | Theoretical prediction         | Cheng et al. (2016b)                           |
|                                 | $b_3 > 0^e$   |                                |  |
| TMI+O <sub>2</sub> <sup>f</sup> | $k_6[\text{H}^+]^{-0.74}[\text{S(IV)}][\text{Mn(II)}][\text{Fe(III)}] (\text{pH} \leq 4.2)$                     |                                | Ibusuki and Takeuchi (1987)                    |
|                                 | $k_6 = 3.72 \times 10^7 \times e^{(-8431.6 \times (1/T - 1/297))} \text{ M}^{-2} \text{ s}^{-1}$                |                                |  |
|                                 | $k_7[\text{H}^+]^{0.67}[\text{S(IV)}][\text{Mn(II)}][\text{Fe(III)}] (\text{pH} > 4.2)$                         |                                |  |
|                                 | $k_7 = 2.51 \times 10^{13} \times e^{(-8431.6 \times (1/T - 1/297))} \text{ M}^{-2} \text{ s}^{-1}$             |                                |  |
|                                 | $\log_{10}\left(\frac{k}{k_{I_s=0}}\right) = \frac{b_4 \sqrt{I_s}}{1 + \sqrt{I_s}}^g$                           | $I_{s, \max} = 2 \text{ M}$    | Martin and Hill (1987, 1967)                   |
|                                 | $b_4$ is in range of -4 to -2   |                                |  |

|                       |  |                     |
|-----------------------|--|---------------------|
| Mn surface            | $k_8 \times f(H^+) \times f(T) \times f(I_s) \times [Mn(II)] \times [SO_2(g)] \times A$<br>$k_8 = 11079.30 \mu\text{g}/\text{m}^3/\text{min}$ , A is the surface area<br>concentration in $\text{nm}^2/\text{cm}^3$ , and the $SO_2$ mixing ratio is in<br>ppbV<br>$f(H^+) = -1 / (1 - 8.83 \times 10^{17} \times [H^+] - 7.84 \times 10^{21} \times [H^+]^2)$<br>$f(T) = e^{-11576.08 \times (1/T - 1/298)}$<br>$f(I_s) = \begin{cases} 1, I_s < 1.52911 \times 10^{-41} \times e^{\frac{T}{2999.19}} + 13.8704 \\ 10.3, I_s \geq 1.52911 \times 10^{-41} \times e^{\frac{T}{2999.19}} + 13.8704 \end{cases}$ | Wang et al. (2020)  |
| Nitrate<br>photolysis | $1.64 \times EF \times [NO_3^-] \times J_{HNO_3} \times \frac{K_{HONO}}{K_{HONO} + [H^+]} \times V \times A \times 0.25 \times [SO_2]$<br>$K_{HONO} = 10^{-3.3} \text{ M}$ , $EF = 1 \sim 100$   | Zheng et al. (2020) |

<sup>a</sup> The aerosol pH was in the range of 4.1 to 5.2 based on the calculations of ISORRPIA II model in winter and 3.8 to 4.9 in summer, which are consistent with the observed in NCP (Liu et al., 2017; Guo et al., 2017).

<sup>b</sup> The values of  $b_1$  and  $b_2$  are different for different solutions (Maahs, 1983; Lagrange et al., 1994). Since these values vary largely and have a significant impact on the estimated reaction rate at high  $I_s$  in aerosol water, we used a medium value of  $b_1 = 1.0$  and  $b_2 = 1.94$  in according to the calculation in Cheng to show the general pattern. Due to the low concentration of  $O_3$  during haze periods, the pathway provides little contribution in the sulfate formation.

<sup>c</sup> The last expression is the fitting results from the measurement results of Liu et al. (2020) Figure S10. The typical enhancement factor of proton-catalyzed sulfate formation rate is 40 in the haze periods of the winter campaign with an averaged ionic strength as 36.3 M.

<sup>d</sup> The  $k_{slow}$  was taken from Lee and Schwartz (1983). They reported a lower-limit value of  $k_{slow} = 2 \times 10^6 \text{ M}^{-1} \text{ s}^{-1}$  at pH of 5.8 and 6.4. The  $k_{high}$  is in the pH range of 5.3–13 as reported by Clifton et al. (1988) and it increases with increasing pH. We used the value  $k_{high} = 1.24 \times 10^7 \text{ M}^{-1} \text{ s}^{-1}$  for  $\text{pH} < 5.3$ , and  $k_{high} = (0.1239 \text{ pH} + 0.5954) \times 10^7 \text{ M}^{-1} \text{ s}^{-1}$  for  $\text{pH}$  in 5.3–7.8 in the present calculations.

<sup>e</sup> The  $b_3$  was predicted theoretically to be positive as 0.5 (Cheng et al., 2016b), however, no specific value of  $b_3$  was determined from laboratory work. Because of the high value of ionic strength during the PKU campaign, we proposed an expression for the activity coefficient of  $NO_2$  based on the Sechenov theory to reflect the trend of its reaction rate increasing with the concentrations and chose  $b_3$  value as 0.01, typical value of activity enhancement of  $NO_2$  with S(IV) is 2.31 with averaged ionic strength equaling to 36.3 during the haze periods. With  $b_3$  equaling to 0.5 proposed in Cheng et al. (2016b), however, typical value is  $1.41 \times 10^{18}$ .

<sup>f</sup> Thus we didn't consider the influence of  $I_s$  on S(IV) +  $NO_2$  in aerosol water in our calculation.

<sup>f</sup> S(IV) oxidation by  $O_2$ , which is via a radical chain mechanism, can be initiated by transition metal ions (TMIs) in bulk water ( $k_6$  and  $k_7$ ). In our calculation, the reaction rate  $k_6$  and  $k_7$  was used for sulfate production via S(IV) +  $O_2$ . Only Fe (III) and Mn (II) are considered here, since other transition metal ions (TMIs), such as Sc (III), Ti (III), V(III), Cr (III), Co (II), Ni (II), Cu

(II) and Zn (II), showed much less catalytic activities (Huss Jr et al., 1982). In addition, it has been concluded that the decreased  
150 temperature would generally lead to a decrease in overall reaction rate. Based on the measurement results of Ibusuki and  
Takeuchi (1987), the correction of temperature are considered in the present study.

<sup>§</sup> Impact of ionic strength on the sulfate formation rate of aqueous phase TMI-catalyzed oxidation of dissolved SO<sub>2</sub> by O<sub>2</sub> in  
aerosol particles was studied by Liu et al. (2020). In their results,  $b_4$  is -3.02 based on the fitting modeling and in the range of  
-2 for Fe(III) and -4 for Mn(II) (Martin and Hill, 1987, 1967). We used  $b_4$  as -3.02 in the calculations in the present study.

155

Table S3. Calculations of Henry' law coefficients and influence of ionic strength.

| Gas species                                | Henry's law coefficient and the influence of $I_s$   | Notes                               | References                                      |
|--|--|-------------------------------------|---|
| SO <sub>2</sub>                            | $H_{\text{SO}_2}^{I_s=0} = 1.23 \times e^{(3145.3 \times (\frac{1}{T} - \frac{1}{298}))}$                        |                                     | Seinfeld and Pandis (2016)                      |
|  | $\log_{10}(\frac{H_{\text{SO}_2}}{H_{\text{SO}_2}^{I_s=0}}) = (\frac{22.3}{T} - 0.0997) \times I_s$              | $I_{s, \text{max}} = 6 \text{ M}$   | Millero et al. (1989)                           |
| O <sub>3</sub>                             | $H_{\text{O}_3} = e^{(\frac{2297}{T} - 2.659 \times I_s + 688 \times \frac{I_s}{T} - 12.19)}$                    | $I_{s, \text{max}} = 0.6 \text{ M}$ | Kosak-Channing and Helz (1983)                  |
| H <sub>2</sub> O <sub>2</sub> <sup>b</sup> | $H_{\text{H}_2\text{O}_2}^{I_s=0} = 1.3 \times 10^5 \times e^{(7297.1 \times (\frac{1}{T} - \frac{1}{292}))}$    |                                     | Seinfeld and Pandis (2016); Chung et al. (2005) |
|  | $\frac{H_{\text{H}_2\text{O}_2}}{H_{\text{H}_2\text{O}_2}^{I_s=0}} = 1 - 1.414 \times 10^{-3} I_s^2 + 0.121 I_s$ | $I_{s, \text{max}} = 5 \text{ M}$   | Liu et al. (2020)                               |
| NO <sub>2</sub> <sup>a</sup>               | $H_{\text{NO}_2}^{I_s=0} = 1.0 \times 10^{-2} \times e^{(2516.2 \times (\frac{1}{T} - \frac{1}{298}))}$          |                                     | Seinfeld and Pandis (2016)                      |

<sup>a</sup> We didn't consider the influence of  $I_s$  on  $H_{\text{NO}_2}$  in our calculation due to the lack of relevant laboratory data.  $H$  is in unit of M atm<sup>-1</sup>.

160 Table S4. Typical activity coefficient values and expressions used in the MARK model

| Species  | Calculation expression or typical value   |
|--|---|
| Inorganic ions   |   |
| H <sup>+</sup>   | 0.4   |
| OH <sup>-</sup>  | 0.5   |
| NH <sub>4</sub> <sup>+</sup>                                     | 0.2   |
| Na <sup>+</sup>  | 0.3   |
| SO <sub>4</sub> <sup>2-</sup>                                    | 0.02  |
| HSO <sub>4</sub> <sup>-</sup>                                    | 1   |
| NO <sub>3</sub> <sup>-</sup>                                     | 0.4   |
| Fe(II), Cu(I), Cu(II), Mn(II) ions and their hydroxides          | $\log_{10}(a_i) = \frac{-z_i^2 \times 0.5109\sqrt{I_s}}{1 + 1.5 \times \sqrt{I_s}}$ |
| Fe(III) and its hydroxides                                       | 0.001   |
| Organic matters and Fe-complex                                   |   |
| H <sub>2</sub> C <sub>2</sub> O <sub>4</sub>                     | 0.6   |
| HC <sub>2</sub> O <sub>4</sub> <sup>-</sup>                      | 0.05  |
| C <sub>2</sub> O <sub>4</sub> <sup>2-</sup>                      | 0.43  |
| [Fe(C <sub>2</sub> O <sub>4</sub> ) <sub>2</sub> ] <sup>-</sup>  | 0.43  |
| [Fe(C <sub>2</sub> O <sub>4</sub> ) <sub>3</sub> ] <sup>3-</sup> | 0.43  |
| [Fe(C <sub>2</sub> O <sub>4</sub> ) <sub>3</sub> ] <sup>3-</sup> | 0.001   |

<sup>a</sup> Non-ideality is treated with the approach by Zuend et al. (2008);Zuend et al. (2011) applied in the AIOMFAC model (Aerosol Inorganic–Organic Mixtures Functional groups Activity Coefficients, <http://www.aiomfac.caltech.edu/index.html>, last access: 18 July 2020).

165 Table S5. Kinetic data for the simulation of reactions in the aerosol particle condensed phase.

| Number           | Reaction  | $k_{298}$ ( $M^{-n+1} s^{-1}$ ) | $Ea/R$ (K) |
|------------------|---|---------------------------------|------------|
| Iron reactions   |   |                                 |            |
| A1               | $Fe^{2+} + H_2O_{2(a)} \rightarrow Fe^{3+} + OH_{(a)} + OH^-$         | 70                              | 5050       |
| A2               | $Fe^{2+} + O_{3(a)} \rightarrow FeO^{2+} + O_{2(a)}$                  | $8.2 \times 10^5$               | 4690       |
| A3               | $FeO^{2+} + H_2O_{2(a)} \rightarrow Fe^{3+} + HO_{2(a)} + OH^-$       | $9.5 \times 10^3$               | 2766       |
| A4               | $FeO^{2+} + HO_{2(a)} \rightarrow Fe^{3+} + O_{2(a)} + OH^-$          | $2 \times 10^6$                 | 0          |
| A5               | $FeO^{2+} + OH_{(a)} + H^+ \rightarrow Fe^{3+} + H_2O_{2(a)}$         | $1 \times 10^7$                 | 0          |
| A6               | $FeO^{2+} + H_2O_{(a)} \rightarrow Fe^{3+} + OH_{(a)} + OH^-$         | $2.3 \times 10^{-2}$            | 4100       |
| A7               | $FeO^{2+} + Fe^{2+} + H_2O_{(a)} \rightarrow 2 Fe^{3+} + 2 OH^+$      | $7.2 \times 10^4$               | 842        |
| A8               | $FeO^{2+} + Fe^{2+} + H_2O_{(a)} \rightarrow Fe(OH)_2Fe^{4+}$         | $1.8 \times 10^4$               | 5052       |
| A9               | $Fe(OH)_2Fe^{4+} + 2 H^+ \rightarrow 2 Fe^{3+} + 2 H_2O_{(a)}$        | 2                               | 5653       |
| A10              | $Fe(OH)_2Fe^{4+} \rightarrow 2 Fe^{3+} + 2 OH^-$                      | 0.49                            | 8780       |
| A11              | $FeO^{2+} + HNO_{2(a)} \rightarrow Fe^{3+} + NO_{2(a)} + OH^-$        | $1.1 \times 10^4$               | 4150       |
| A12              | $FeO^{2+} + H^+ + NO_2^- \rightarrow Fe^{3+} + NO_{2(a)} + OH^-$      | $2.5 \times 10^5$               | 0          |
| A13              | $FeO^{2+} + HSO_3^- \rightarrow Fe^{3+} + OH^- + SO_3^-$              | $1 \times 10^5$                 | 0          |
| A14              | $Fe^{2+} + OH_{(a)} \rightarrow Fe(OH)^{2+}$                          | $4.3 \times 10^8$               | 1100       |
| A15              | $Fe(OH)^{2+} + HO_{2(a)} \rightarrow Fe^{2+} + O_{2(a)} + H_2O_{(a)}$ | $1.3 \times 10^5$               | 0          |
| A16              | $Fe(OH)^{2+} + O_2 \rightarrow Fe^{2+} + O_{2(a)} + OH^-$             | $1.5 \times 10^8$               | 0          |
| A17              | $Fe^{3+} + O_2^- \rightarrow Fe^{2+} + O_{2(a)}$                      | $1.5 \times 10^8$               | 0          |
| A18              | $Fe^{2+} + 2 H^+ + O_2^- \rightarrow Fe^{3+} + H_2O_{2(a)}$           | $1 \times 10^7$                 | 0          |
| A19              | $Fe^{2+} + HO_{2(a)} + H^+ \rightarrow Fe^{3+} + H_2O_{2(a)}$         | $1.2 \times 10^6$               | 5050       |
| A20              | $Fe(OH)_2^+ + O_2^- \rightarrow Fe^{2+} + O_{2(a)} + 2 OH^-$          | $1.5 \times 10^8$               | 0          |
| A21              | $Fe(OH)^{2+} + HSO_3^- \rightarrow Fe^{2+} + SO_3^- + H_2O_{(a)}$     | 30                              | 0          |
| A22              | $Fe^{2+} + SO_5^- + H_2O_{(a)} \rightarrow Fe(OH)^{2+} + HSO_5^-$     | $2.65 \times 10^7$              | 5809       |
| A23              | $Fe^{2+} + HSO_5^- \rightarrow Fe(OH)^{2+} + SO_4^-$                  | $3 \times 10^4$                 | 0          |
| A24              | $Fe^{2+} + SO_4^- \rightarrow Fe^{3+} + SO_4^{2-}$                    | $4.6 \times 10^9$               | -2165      |
| A25              | $Fe^{2+} + S_2O_8^{2-} \rightarrow Fe^{3+} + SO_4^- + SO_4^{2-}$      | 17                              | 0          |
| Copper reactions |   |                                 |            |
| A26              | $Cu^+ + 2 H^+ + O_2^- \rightarrow Cu^{2+} + H_2O_{2(a)}$              | $8 \times 10^9$                 | 0          |



|                                  |  |                    |      |
|----------------------------------|--|--------------------|------|
| A27                              | $\text{Cu}^+ + \text{HO}_{2(\text{a})} + \text{H}^+ \rightarrow \text{Cu}^{2+} + \text{H}_2\text{O}_{2(\text{a})}$                             | $2.2 \times 10^9$  | 0    |
| A28                              | $\text{Cu}^+ + \text{OH}_{(\text{a})} \rightarrow \text{Cu}^{2+} + \text{OH}^-$  | $3 \times 10^9$    | 0    |
| A29                              | $\text{Cu}^{2+} + \text{HO}_{2(\text{a})} \rightarrow \text{Cu}^+ + \text{H}^+ + \text{O}_{2(\text{a})}$                                       | $1 \times 10^8$    | 0    |
| A30                              | $\text{Cu}^{2+} + \text{O}_2^- \rightarrow \text{Cu}^+ + \text{O}_{2(\text{a})}$   | $1 \times 10^9$    | 0    |
| A31                              | $\text{Cu}^+ + \text{O}_{2(\text{a})} \rightarrow \text{Cu}^{2+} + \text{O}_2^-$   | $4.6 \times 10^5$  | 0    |
| A32                              | $\text{Cu}^+ + \text{H}^+ + \text{O}_{3(\text{a})} \rightarrow \text{Cu}^{2+} + \text{O}_{2(\text{a})} + \text{OH}_{(\text{a})}$               | $3 \times 10^7$    | 0    |
| A33                              | $\text{Cu}^+ + \text{H}_2\text{O}_{2(\text{a})} \rightarrow \text{Cu}^{2+} + \text{OH}_{(\text{a})} + \text{OH}^-$                             | $7 \times 10^3$    | 0    |
| A34                              | $\text{Cu}^+ + \text{SO}_4^- \rightarrow \text{Cu}^{2+} + \text{SO}_4^{2-}$  | $3 \times 10^8$    | 0    |
| <b>Mn reactions</b>              |  |                    |      |
| A35                              | $\text{Mn}^{4+} + \text{H}_2\text{O}_{2(\text{a})} \rightarrow \text{Mn}^{2+} + \text{O}_{2(\text{a})} + 2\text{H}^+$                          | $7.3 \times 10^4$  | 0    |
| A36                              | $\text{Mn}^{3+} + \text{H}_2\text{O}_{2(\text{a})} \rightarrow \text{Mn}^{2+} + \text{HO}_{2(\text{a})} + \text{H}^+$                          | $7.3 \times 10^4$  | 0    |
| A37                              | $\text{MnOH}^{2+} + \text{H}_2\text{O}_{2(\text{a})} \rightarrow \text{MnO}_2^+ + \text{H}^+$  | $2.8 \times 10^3$  | 0    |
| A38                              | $\text{MnO}_2^+ + \text{HO}_{2(\text{a})} + \text{H}^+ \rightarrow \text{H}_2\text{O}_{2(\text{a})} + \text{Mn}^{2+} + \text{O}_{2(\text{a})}$ | $1 \times 10^7$    | 0    |
| A39                              | $\text{Mn}^{2+} + \text{OH}_{(\text{a})} \rightarrow \text{Mn}^{3+} + \text{OH}^-$   | $3.4 \times 10^7$  | 0    |
| A40                              | $2 \text{MnO}_2^+ + 2\text{H}^+ \rightarrow 2\text{Mn}^{2+} + \text{H}_2\text{O}_{2(\text{a})}$  | $6 \times 10^6$    | 0    |
| A41                              | $\text{MnO}^{2+} + 2\text{H}^+ + \text{Mn}^{2+} \rightarrow 2\text{Mn}^{3+}$   | $1 \times 10^5$    | 0    |
| A42                              | $\text{Mn}^{2+} + \text{O}_{3(\text{a})} + \text{H}^+ \rightarrow \text{Mn}^{3+} + \text{O}_{2(\text{a})} + \text{OH}_{(\text{a})}$            | $1.65 \times 10^5$ | 0    |
| A43                              | $\text{Mn}^{2+} + \text{NO}_{3(\text{a})} \rightarrow \text{Mn}^{3+} + \text{NO}_3^-$  | $1.5 \times 10^6$  | 0    |
| A44                              | $\text{Mn}^{2+} + \text{HSO}_5^- \rightarrow \text{Mn}^{3+} + \text{SO}_4^- + \text{OH}^-$   | $3 \times 10^4$    | 0    |
| A45                              | $\text{Mn}^{2+} + \text{SO}_5^- \rightarrow \text{Mn}^{3+} + \text{HSO}_5^- + \text{OH}^-$   | $1 \times 10^{10}$ | 0    |
| A46                              | $\text{Mn}^{2+} + \text{SO}_4^- \rightarrow \text{Mn}^{3+} + \text{SO}_4^{2-}$   | $1.4 \times 10^7$  | 4089 |
| A47                              | $\text{MnHSO}_3^+ + \text{Mn}^{3+} \rightarrow \text{H}^+ + 2\text{Mn}^{2+} + \text{SO}_3^-$   | $1.3 \times 10^6$  | 0    |
| <b>Cu-Fe-Mn redox reactions</b>  |  |                    |      |
| A48                              | $\text{Cu}^+ + \text{Fe}^{3+} \rightarrow \text{Cu}^{2+} + \text{Fe}^{2+}$   | $1.3 \times 10^7$  | 0    |
| A49                              | $\text{Cu}^+ + \text{FeOH}^{2+} \rightarrow \text{Cu}^{2+} + \text{Fe}^{2+} + \text{OH}^-$   | $1.3 \times 10^7$  | 0    |
| A50                              | $\text{Cu}^+ + \text{Fe}(\text{OH})_2^+ \rightarrow \text{Cu}^{2+} + \text{Fe}^{2+} + 2 \text{OH}^-$   | $1.3 \times 10^7$  | 0    |
| A51                              | $\text{Mn}^{3+} + \text{Fe}^{2+} \rightarrow \text{Mn}^{2+} + \text{Fe}^{3+}$  | $1.6 \times 10^4$  | 0    |
| A52                              | $\text{Mn}^{2+} + \text{FeO}^{2+} + 2\text{H}^+ \rightarrow \text{Mn}^{3+} + \text{Fe}^{3+}$   | $1 \times 10^4$    | 2562 |
| <b>Hydroxide redox reactions</b> |  |                    |      |
| A53                              | $\text{O}_2^- + \text{O}_{3(\text{a})} \rightarrow \text{O}_{2(\text{a})} + \text{O}_3^-$  | $1.5 \times 10^9$  | 2200 |

|                                       |  |                      |      |
|---------------------------------------|--|----------------------|------|
| A54                                   | $2 \text{HO}_{2(a)} \rightarrow \text{H}_2\text{O}_{2(a)} + \text{O}_{2(a)}$   | $8.3 \times 10^5$    | 2700 |
| A55                                   | $\text{HO}_{2(a)} + \text{O}_2^- + \text{H}_2\text{O}_{(a)} \rightarrow \text{H}_2\text{O}_{2(a)} + \text{O}_{2(a)} + \text{OH}^-$ | $9.7 \times 10^7$    | 1060 |
| A56                                   | $\text{HO}_{2(a)} + \text{OH}_{(a)} \rightarrow \text{O}_{2(a)} + \text{H}_2\text{O}_{(a)}$  | $1 \times 10^{10}$   | 0    |
| A57                                   | $\text{O}_2^- + \text{OH}_{(a)} \rightarrow \text{O}_{2(a)} + \text{OH}^-$   | $1.1 \times 10^{10}$ | 2120 |
| A58                                   | $\text{H}_2\text{O}_{2(a)} + \text{OH}_{(a)} \rightarrow \text{HO}_{2(a)} + \text{H}_2\text{O}_{(a)}$                              | $3 \times 10^7$      | 1680 |
| Organic reactions                     |  |                      |      |
| A59                                   | $\text{H}_2\text{C}_2\text{O}_4 + \text{OH}_{(a)} \rightarrow \text{H}_2\text{O}_{(a)} + \text{C}_2\text{O}_4^- + \text{H}^+$      | $1.9 \times 10^8$    | 2800 |
| A60                                   | $\text{C}_2\text{O}_4^{2-} + \text{OH}_{(a)} \rightarrow \text{OH}^- + \text{C}_2\text{O}_4^-$                                     | $1.6 \times 10^8$    | 4300 |
| A61                                   | $\text{C}_2\text{O}_4^- + \text{O}_{2(a)} \rightarrow 2 \text{CO}_{2(a)} + \text{O}_2^-$   | $2 \times 10^9$      | 2800 |
| A62                                   | $\text{HC}_2\text{O}_4^- + \text{SO}_3^- \rightarrow \text{C}_2\text{O}_4^- + \text{HSO}_3^-$                                      | $5 \times 10^3$      | 0    |
| A63                                   | $\text{HC}_2\text{O}_4^- + \text{SO}_4^- \rightarrow \text{C}_2\text{O}_4^- + \text{H}^+ + \text{SO}_4^{2-}$                       | $3.35 \times 10^5$   | 0    |
| A64                                   | $\text{HC}_2\text{O}_4^- + \text{NO}_{3(a)} \rightarrow \text{C}_2\text{O}_4^- + \text{H}^+ + \text{NO}_3^-$                       | $6.8 \times 10^7$    | 0    |
| A65                                   | $\text{C}_2\text{O}_4^{2-} + \text{H}^+ + \text{SO}_3^- \rightarrow \text{C}_2\text{O}_4^- + \text{HSO}_3^-$                       | $1 \times 10^4$      | 0    |
| A66                                   | $\text{C}_2\text{O}_4^{2-} + \text{SO}_4^- \rightarrow \text{C}_2\text{O}_4^- + \text{SO}_4^{2-}$                                  | $1.05 \times 10^6$   | 0    |
| A67                                   | $\text{C}_2\text{O}_4^{2-} + \text{NO}_{3(a)} \rightarrow \text{C}_2\text{O}_4^- + \text{NO}_3^-$                                  | $2.2 \times 10^8$    | 0    |
| A68                                   | $\text{HCOOH} + \text{OH} (+\text{O}_2) \rightarrow \text{Products}$   | $3.2 \times 10^9$    | 0    |
| Fe-oxalate complex reactions          |  |                      |      |
| A69                                   | $\text{Fe}^{2+} + \text{C}_2\text{O}_4^{2-} \rightarrow \text{FeC}_2\text{O}_{4(a)}$   | $1 \times 10^6$      | 0    |
| A70                                   | $\text{FeC}_2\text{O}_{4(a)} \rightarrow \text{Fe}^{2+} + \text{C}_2\text{O}_4^{2-}$   | $1 \times 10^3$      | 0    |
| A71                                   | $\text{FeC}_2\text{O}_4^+ + \text{O}_2^- \rightarrow \text{FeC}_2\text{O}_{4(a)} + \text{O}_{2(a)}$                                | $1 \times 10^6$      | 0    |
| A72                                   | $\text{FeC}_2\text{O}_4^+ + \text{HO}_{2(a)} \rightarrow \text{FeC}_2\text{O}_{4(a)} + \text{O}_{2(a)} + \text{H}^+$               | $1.2 \times 10^5$    | 0    |
| Sulfur and Nitrate compound reactions |  |                      |      |
| A73                                   | $\text{HSO}_3^- + \text{OH}_{(a)} \rightarrow \text{SO}_3^- + \text{H}_2\text{O}_{(a)}$  | $2.7 \times 10^9$    | 0    |
| A74                                   | $\text{OH}_{(a)} + \text{SO}_3^{2-} \rightarrow \text{OH}^- + \text{SO}_3^-$   | $4.6 \times 10^9$    | 0    |
| A75                                   | $\text{H}_2\text{O}_{(a)} + \text{N}_2\text{O}_{5(a)} \rightarrow 2 \text{H}^+ + 2 \text{NO}_3^-$                                  | $5 \times 10^9$      | 0    |
| A76                                   | $\text{N}_2\text{O}_{5(a)} \rightarrow \text{NO}_2^+ + \text{NO}_3^-$  | $1 \times 10^9$      | 0    |
| A77                                   | $\text{H}_2\text{O}_{(a)} + \text{NO}_2^+ \rightarrow 2 \text{H}^+ + \text{NO}_3^-$  | $8.9 \times 10^7$    | 0    |
| A78                                   | $\text{Fe}^{2+} + \text{NO}_{3(a)} \rightarrow \text{Fe}^{3+} + \text{NO}_3^-$   | $8 \times 10^6$      | 0    |
| A79                                   | $\text{H}_2\text{O}_{2(a)} + \text{NO}_{3(a)} \rightarrow \text{HO}_{2(a)} + \text{H}^+ + \text{NO}_3^-$                           | $4.9 \times 10^6$    | 2000 |
| A80                                   | $\text{HO}_{2(a)} + \text{NO}_{3(a)} \rightarrow \text{H}^+ + \text{NO}_3^- + \text{O}_{2(a)}$                                     | $3 \times 10^9$      | 0    |

|      |  |                      |       |
|------|--|----------------------|-------|
| A81  | $\text{NO}_{3(a)} + \text{O}_2^- \rightarrow \text{NO}_3^- + \text{O}_{2(a)}$                              | $3 \times 10^9$      | 0     |
| A82  | $\text{HSO}_3^- + \text{NO}_{3(a)} \rightarrow \text{H}^+ + \text{NO}_3^- + \text{SO}_3^-$                 | $1.3 \times 10^9$    | 2000  |
| A83  | $\text{NO}_{3(a)} + \text{SO}_3^{2-} \rightarrow \text{NO}_3^- + \text{SO}_3^-$                            | $3 \times 10^8$      | 0     |
| A84  | $\text{HSO}_4^- + \text{NO}_{3(a)} \rightarrow \text{H}^+ + \text{NO}_3^- + \text{SO}_4^-$                 | $2.6 \times 10^5$    | 0     |
| A85  | $\text{NO}_{3(a)} + \text{SO}_4^{2-} \rightarrow \text{NO}_3^- + \text{SO}_4^-$                            | $1 \times 10^5$      | 0     |
| A86  | $\text{NO}_{2(a)} + \text{OH}_{(a)} \rightarrow \text{HOONO}_{(a)}$  | $1.2 \times 10^{10}$ | 0     |
| A87  | $\text{NO}_{2(a)} + \text{O}_2^- \rightarrow \text{NO}_2^- + \text{O}_{2(a)}$                              | $1 \times 10^8$      | 0     |
| A88  | $2 \text{NO}_{2(a)} + \text{H}_2\text{O}_{(a)} \rightarrow \text{HNO}_{2(a)} + \text{H}^+ + \text{NO}_3^-$ | $8.4 \times 10^7$    | -2900 |
| A89  | $\text{NO}_2^- + \text{OH}_{(a)} \rightarrow \text{NO}_{2(a)} + \text{OH}^-$                               | $9.1 \times 10^9$    | 0     |
| A90  | $\text{NO}_2^- + \text{SO}_4^- \rightarrow \text{NO}_{2(a)} + \text{SO}_4^{2-}$                            | $7.2 \times 10^8$    | 0     |
| A91  | $\text{NO}_2^- + \text{NO}_{3(a)} \rightarrow \text{NO}_{2(a)} + \text{NO}_3^-$                            | $1.4 \times 10^9$    | 0     |
| A92  | $\text{NO}_2^- + \text{O}_{3(a)} \rightarrow \text{NO}_3^- + \text{O}_{2(a)}$                              | $5 \times 10^5$      | 6900  |
| A93  | $\text{HNO}_{2(a)} + \text{OH}_{(a)} \rightarrow \text{NO}_{2(a)} + \text{H}_2\text{O}_{(a)}$              | $1.1 \times 10^{10}$ | 0     |
| A94  | $\text{HNO}_{4(a)} + \text{HSO}_3^- \rightarrow \text{HSO}_4^- + \text{H}^+ + \text{NO}_3^-$               | $3.3 \times 10^5$    | 0     |
| A95  | $\text{H}_2\text{O}_{(a)} + \text{SO}_{3(a)} \rightarrow 2 \text{H}^+ + \text{SO}_4^{2-}$                  | $1 \times 10^{10}$   | 0     |
| A96  | $\text{O}_{3(a)} + \text{SO}_3^{2-} \rightarrow \text{O}_{2(a)} + \text{SO}_4^{2-}$                        | $1.5 \times 10^9$    | 5280  |
| A97  | $2 \text{SO}_5^- \rightarrow \text{O}_{2(a)} + \text{S}_2\text{O}_8^{2-}$                                  | $4.8 \times 10^7$    | 2600  |
| A98  | $2 \text{SO}_5^- \rightarrow \text{O}_{2(a)} + 2 \text{SO}_4^-$  | $2.2 \times 10^8$    | 2600  |
| A99  | $\text{H}^+ + \text{O}_2^- + \text{SO}_5^- \rightarrow \text{HSO}_5^- + \text{O}_{2(a)}$                   | $2.34 \times 10^8$   | 0     |
| A100 | $\text{O}_{2(a)} + \text{SO}_{3(a)} \rightarrow \text{SO}_5^-$   | $2.5 \times 10^9$    | 0     |
| A101 | $\text{HSO}_3^- + \text{SO}_5^- \rightarrow \text{HSO}_5^- + \text{SO}_3^-$                                | $8.6 \times 10^3$    | 0     |
| A102 | $\text{HSO}_3^- + \text{SO}_5^- \rightarrow \text{H}^+ + \text{SO}_4^- + \text{SO}_4^{2-}$                 | $3.6 \times 10^2$    | 0     |
| A103 | $\text{H}^+ + \text{SO}_3^{2-} + \text{SO}_5^- \rightarrow \text{HSO}_5^- + \text{SO}_3^-$                 | $2.1 \times 10^5$    | 0     |
| A104 | $\text{SO}_3^{2-} + \text{SO}_5^- \rightarrow \text{SO}_4^- + \text{SO}_4^{2-}$                            | $5.5 \times 10^5$    | 0     |
| A105 | $\text{HSO}_4^- + \text{OH}_{(a)} \rightarrow \text{SO}_4^- + \text{H}_2\text{O}_{(a)}$                    | $3.5 \times 10^5$    | 0     |
| A106 | $2 \text{SO}_4^- \rightarrow \text{S}_2\text{O}_8^{2-}$  | $6.1 \times 10^8$    | 840   |
| A107 | $\text{HSO}_3^- + \text{SO}_4^- \rightarrow \text{H}^+ + \text{SO}_3^- + \text{SO}_4^{2-}$                 | $5.8 \times 10^8$    | 0     |
| A108 | $\text{SO}_3^{2-} + \text{SO}_4^- \rightarrow \text{SO}_3^- + \text{SO}_4^{2-}$                            | $3.4 \times 10^8$    | 1200  |
| A109 | $\text{H}_2\text{O}_{2(a)} + \text{SO}_4^- \rightarrow \text{HO}_{2(a)} + \text{H}^+ + \text{SO}_4^{2-}$   | $1.7 \times 10^7$    | 0     |
| A110 | $\text{HO}_{2(a)} + \text{SO}_4^- \rightarrow \text{H}^+ + \text{O}_{2(a)} + \text{SO}_4^{2-}$             | $3.5 \times 10^9$    | 0     |

|      |  |                    |      |
|------|--|--------------------|------|
| A111 | $\text{O}_2^- + \text{SO}_4^- \rightarrow \text{O}_{2(a)} + \text{SO}_4^{2-}$  | $3.5 \times 10^9$  | 0    |
| A112 | $\text{NO}_3^- + \text{SO}_4^- \rightarrow \text{NO}_{3(a)} + \text{SO}_4^{2-}$  | $5 \times 10^4$    | 0    |
| A113 | $\text{OH}^- + \text{SO}_4^- \rightarrow \text{OH}_{(a)} + \text{SO}_4^{2-}$   | $1.4 \times 10^7$  | 0    |
| A114 | $\text{H}_2\text{O}_{(a)} + \text{SO}_4^- \rightarrow \text{H}^+ + \text{OH}_{(a)} + \text{SO}_4^{2-}$                           | 11                 | 1100 |
| A115 | $\text{HSO}_3^- + \text{HSO}_5^- + \text{H}^+ \rightarrow 3 \text{H}^+ + 2 \text{SO}_4^{2-}$                                     | $7.14 \times 10^6$ | 0    |
| A116 | $\text{SO}_3^{2-} + \text{HSO}_5^- + \text{H}^+ \rightarrow 2 \text{H}^+ + 2 \text{SO}_4^{2-}$                                   | $7.14 \times 10^6$ | 0    |
| A117 | $\text{HSO}_5^- + \text{OH}_{(a)} \rightarrow \text{SO}_5^- + \text{H}_2\text{O}_{(a)}$  | $1.7 \times 10^7$  | 0    |
| A118 | $\text{OH}_{(a)} + \text{SO}_4^- \rightarrow \text{HSO}_5^-$   | $1 \times 10^{10}$ | 0    |
| A119 | $\text{H}_2\text{O}_{2(a)} + \text{HSO}_3^- + \text{H}^+ \rightarrow 2 \text{H}^+ + \text{SO}_4^{2-} + \text{H}_2\text{O}_{(a)}$ | $7.2 \times 10^7$  | 4000 |
| A120 | $\text{O}_{3(a)} + \text{SO}_{2(a)} + \text{H}_2\text{O}_{(a)} \rightarrow \text{HSO}_4^- + \text{H}^+ + \text{O}_{2(a)}$        | $2.4 \times 10^4$  | 0    |
| A121 | $\text{HSO}_3^- + \text{O}_{3(a)} \rightarrow \text{SO}_4^{2-} + \text{H}^+ + \text{O}_{2(a)}$                                   | $3.7 \times 10^5$  | 5530 |
| A122 | $\text{NO}_{3(a)} + \text{OH}^- \rightarrow \text{NO}_3^- + \text{OH}_{(a)}$   | $9.4 \times 10^7$  | 2700 |

Table S6. Photolysis rates (aqueous phase) used in the model at noon (sza = 20°)

| Number | Reaction  | $J_0$ (s <sup>-1</sup> ) |
|--------|---|--------------------------|
| J1     | $\text{H}_2\text{O}_{2(a)} + h\nu \rightarrow 2 \text{OH}_{(a)}$  | $6.98 \times 10^{-6}$    |
| J2     | $\text{Fe}^{3+} + \text{H}_2\text{O}_{(a)} + h\nu \rightarrow \text{Fe}^{2+} + \text{OH}_{(a)} + \text{H}^+$                        | $9.3 \times 10^{-6}$     |
| J3     | $\text{Fe}(\text{OH})^{2+} + h\nu \rightarrow \text{Fe}^{2+} + \text{OH}_{(a)}$   | $4.39 \times 10^{-3}$    |
| J4     | $\text{Fe}(\text{OH})_2^+ + h\nu \rightarrow \text{Fe}^{2+} + \text{OH}_{(a)} + \text{OH}^-$  | $5.63 \times 10^{-3}$    |
| J5     | $\text{NO}_2 + h\nu \rightarrow \text{NO}_{(a)} + \text{OH}_{(a)}$  | $2.51 \times 10^{-5}$    |
| J6     | $\text{NO}_3 + h\nu \rightarrow \text{NO}_{2(a)} + \text{OH}_{(a)}$   | $4.15 \times 10^{-7}$    |
| J7     | $\text{Fe}[(\text{C}_2\text{O}_4)_2]^- + h\nu \rightarrow \text{C}_2\text{O}_4^{2-} + \text{C}_2\text{O}_4^- + \text{Fe}^{2+}$      | $2.30 \times 10^{-2}$    |
| J8     | $\text{Fe}[(\text{C}_2\text{O}_4)_3]^{3-} + h\nu \rightarrow 2 \text{C}_2\text{O}_4^{2-} + \text{C}_2\text{O}_4^- + \text{Fe}^{2+}$ | $5.76 \times 10^{-2}$    |
| J9     | $\text{FeC}_2\text{O}_4^+ + h\nu \rightarrow \text{Fe}^{2+} + \text{C}_2\text{O}_4^-$   | $7.20 \times 10^{-4}$    |
| J10    | $\text{NO}_{3(a)} + h\nu \rightarrow \text{NO}_{(a)} + \text{O}_{2(a)}$   | $2.32 \times 10^{-2*}$   |
| J11    | $\text{NO}_{3(a)} + h\nu \rightarrow \text{NO}_{2(a)} + \text{O}_{(a)}^{3p}$  | $2.01 \times 10^{-1*}$   |

\*Estimated as in the gas phase

Table S7. Aqueous equilibrium reactions

| Number | Reaction   | $K_{298}$ (M)         | $k_{298}$ ( $M^{-n} s^{-1}$ ) |          | $E_a/R$ (K)          | $k_{298}$ ( $M^{-n} s^{-1}$ ) | $E_a/R$ (K) |
|--------|--|-----------------------|-------------------------------|----------|----------------------|-------------------------------|-------------|
|        |  |                       | forward                       | backward |                      |                               |             |
| E1     | $H_2O_{(a)} \leftrightarrow H^+ + OH^-$                          | $1.8 \times 10^{-16}$ | $2.34 \times 10^{-5}$         | 6800     | $1.3 \times 10^{11}$ | 0                             |             |
| E2     | $NH_{3(a)} + H_2O_{(a)} \leftrightarrow NH_4^+ + OH^-$           | $1.17 \times 10^{-5}$ | $6.02 \times 10^5$            | 560      | $3.4 \times 10^{10}$ |                               |             |
| E3     | $HO_{2(a)} \leftrightarrow H^+ + O_2^-$                          | $1.6 \times 10^{-5}$  | $8.0 \times 10^5$             | 0        | $5 \times 10^{10}$   | 0                             |             |
| E4     | $HNO_{3(a)} \leftrightarrow H^+ + NO_3^-$                        | 22                    | $1.1 \times 10^{12}$          | -1800    | $5 \times 10^{10}$   |                               |             |
| E5     | $HNO_{2(a)} \leftrightarrow H^+ + NO_2^-$                        | $5.30 \times 10^{-4}$ | $2.65 \times 10^7$            | 1760     | $5 \times 10^{10}$   |                               |             |
| E6     | $HNO_{4(a)} \leftrightarrow H^+ + O_2NO_2^-$                     | $1 \times 10^{-5}$    | $5 \times 10^5$               |          | $5 \times 10^{10}$   |                               |             |
| E7     | $HO_{2(a)} + NO_{2(a)} \leftrightarrow HNO_{4(a)}$               | $2.17 \times 10^9$    | $1 \times 10^7$               |          | $4.6 \times 10^{-3}$ |                               |             |
| E8     | $HO_{2(a)} + SO_{2(a)} \leftrightarrow HSO_3^- + H^+$            | $3.14 \times 10^{-4}$ | $6.27 \times 10^4$            | -1940    | $2.0 \times 10^8$    |                               |             |
| E9     | $HSO_3^- \leftrightarrow H^+ + SO_3^{2-}$                        | $6.22 \times 10^{-8}$ | 3110                          | -1960    | $5 \times 10^{10}$   |                               |             |
| E10    | $H_2SO_{4(a)} \leftrightarrow HSO_4^- + H^+$                     | $1 \times 10^3$       | $5 \times 10^{13}$            |          | $5 \times 10^{10}$   |                               |             |
| E11    | $HSO_4^- \leftrightarrow H^+ + SO_4^{2-}$                        | $1.02 \times 10^{-2}$ | $1.02 \times 10^9$            | -2700    | $1 \times 10^{11}$   |                               |             |
| E12    | $Fe^{3+} + H_2O_{(a)} \leftrightarrow Fe(OH)^{2+} + H^+$         | $1.09 \times 10^{-4}$ | $4.7 \times 10^4$             |          | $4.3 \times 10^8$    |                               |             |
| E13    | $Fe(OH)^{2+} + H_2O_{(a)} \leftrightarrow Fe(OH)_2^+ + H^+$      | $1.38 \times 10^{-7}$ | $1.1 \times 10^3$             |          | $8 \times 10^9$      |                               |             |
| E14    | $Fe^{3+} + SO_4^{2-} \leftrightarrow Fe(SO_4)^+$                 | $1.78 \times 10^{-2}$ | $3.2 \times 10^3$             |          | $1.8 \times 10^5$    |                               |             |
| E15    | $Cu^{2+} + OH_{(a)} \leftrightarrow Cu(OH)^{2+}$                 | $1.17 \times 10^4$    | $3.5 \times 10^8$             |          | $3 \times 10^4$      |                               |             |
| E16    | $HO_{3(a)} \leftrightarrow H^+ + O_3^-$                          | $5 \times 10^{-9}$    | 330                           |          | $5.2 \times 10^{10}$ |                               |             |
| E17    | $HOONO_{(a)} \leftrightarrow H^+ + OONO^-$                       | $1 \times 10^{-6}$    | $5 \times 10^4$               |          | $5 \times 10^{10}$   |                               |             |
| E18    | $Fe(C_2O_4)^+ \leftrightarrow C_2O_4^{2-} + Fe^{3+}$             | $4.0 \times 10^{-10}$ | $3 \times 10^{-3}$            |          | $7.5 \times 10^6$    |                               |             |
| E19    | $Fe(C_2O_4)_2^- \leftrightarrow C_2O_4^{2-} + Fe(C_2O_4)^+$      | $1.59 \times 10^{-7}$ | $3 \times 10^{-3}$            |          | $1.89 \times 10^4$   |                               |             |
| E20    | $Fe(C_2O_4)_3^{3-} \leftrightarrow C_2O_4^{2-} + Fe(C_2O_4)_2^-$ | $2.65 \times 10^{-5}$ | $3 \times 10^{-3}$            |          | 114                  |                               |             |

Table S8. Kinetic data for the simulation of gas-liquid phase conversion reactions

| Number | Reaction*   | $k_{298}$ ( $M^{-n+1}$ s <sup>-1</sup> )          |   |
|--------|---|---|---|
|        |   | forward   | backward  |
| T1     | $\text{CO}_2(\text{g}) \leftrightarrow \text{CO}_2(\text{a})$                   | $k_{mt \text{ CO}_2} \times \text{ALWC}$          | $k_{mt \text{ CO}_2} / (H_{\text{CO}_2} \text{RT})$                   |
| T2     | $\text{NH}_3(\text{g}) \leftrightarrow \text{NH}_3(\text{a})$                   | $k_{mt \text{ NH}_3} \times \text{ALWC}$          | $k_{mt \text{ NH}_3} / (H_{\text{NH}_3} \text{RT})$                   |
| T3     | $\text{O}_3(\text{g}) \leftrightarrow \text{O}_3(\text{a})$                     | $k_{mt \text{ O}_3} \times \text{ALWC}$           | $k_{mt \text{ O}_3} / (H_{\text{O}_3} \text{RT})$                     |
| T4     | $\text{HO}_2(\text{g}) \leftrightarrow \text{HO}_2(\text{a})$                   | $k_{mt \text{ HO}_2} \times \text{ALWC}$          | $k_{mt \text{ HO}_2} / (H_{\text{HO}_2} \text{RT})$                   |
| T5     | $\text{OH}(\text{g}) \leftrightarrow \text{OH}(\text{a})$                       | $k_{mt \text{ OH}} \times \text{ALWC}$            | $k_{mt \text{ OH}} / (H_{\text{OH}} \text{RT})$                       |
| T6     | $\text{H}_2\text{O}_2(\text{g}) \leftrightarrow \text{H}_2\text{O}_2(\text{a})$ | $k_{mt \text{ H}_2\text{O}_2} \times \text{ALWC}$ | $k_{mt \text{ H}_2\text{O}_2} / (H_{\text{H}_2\text{O}_2} \text{RT})$ |
| T7     | $\text{NO}_3(\text{g}) \leftrightarrow \text{NO}_3(\text{a})$                   | $k_{mt \text{ NO}_3} \times \text{ALWC}$          | $k_{mt \text{ NO}_3} / (H_{\text{NO}_3} \text{RT})$                   |
| T8     | $\text{N}_2\text{O}_5(\text{g}) \leftrightarrow \text{N}_2\text{O}_5(\text{a})$ | $k_{mt \text{ N}_2\text{O}_5} \times \text{ALWC}$ | $k_{mt \text{ N}_2\text{O}_5} / (H_{\text{N}_2\text{O}_5} \text{RT})$ |
| T9     | $\text{NO}_2(\text{g}) \leftrightarrow \text{NO}_2(\text{a})$                   | $k_{mt \text{ NO}_2} \times \text{ALWC}$          | $k_{mt \text{ NO}_2} / (H_{\text{NO}_2} \text{RT})$                   |
| T10    | $\text{SO}_2(\text{g}) \leftrightarrow \text{SO}_2(\text{a})$                   | $k_{mt \text{ SO}_2} \times \text{ALWC}$          | $k_{mt \text{ SO}_2} / (H_{\text{SO}_2} \text{RT})$                   |

175 \* $k_{mt}$  is related to the particle diameters and the aerosol liquid water in different diameter bins. For this reason, the mass transfer rates are corrected by the particle 11 bins diameters in the two field campaigns. The rate  $k_{mt}$  equals to  $\sum_i^{11} k_{mt\_i} \times L_i$

Table S9. Concentration of transition metals in PM<sub>2.5</sub> in urban areas.

| Sampling site           | Period          | Method  | Fe   | Mn   | Cu   | References             |
|-------------------------|-----------------|---------|------|------|------|------------------------|
| China, Beijing, Urban   | 2018.8-2019.8   | XRF     | 596  | 27.9 | 7.37 | Zhao et al. (2021)     |
| China, Beijing, Urban   | 2015.9-2016.1   | XRF     | 686  | 60.2 | 25.1 | Zhang et al. (2019)    |
| China, Beijing, Urban   | 2016.6-2017.5   | ED-XRF  | 738  | 37   | 32   | Cui et al. (2019)      |
| China, Beijing, Urban   | 2014.1-10       | ICP-AES | 1650 | 55   | 108  | Gao et al. (2018)      |
| China, Beijing, Urban   | 2016.1-2017.5   | XRF     | 629  | 32   | 24   | Cui et al. (2020)      |
| China, Beijing, Urban   | 2016.1          | ICP-AES | 2823 | 92.3 | 48   | Duan et al. (2012)     |
| China, Zhengzhou, Urban | 2017.10-2018.7  | XRF     | 1361 | 157  | 29.2 | He et al. (2019)       |
| China, Nanjing, Urban   | 2016.12-2017.12 | XRF     | 577  | 48.9 | 27.2 | Yu et al. (2019)       |
| China, Shanghai, Urban  | 2016.3-2017.2   | ED-XRF  | 410  | 32   | 12   | Chang et al. (2017)    |
| Canada, Hamilton, Urban | 2014.1-2017.6   | XRF     | 49.6 | 0.83 | 2.76 | Sofowote et al. (2019) |
| India, New Delhi, Urban | 2013.1-2016.12  | WD-XRF  | 780  | 10   | 100  | Jain et al. (2020)     |



## SI References

- Ali, H. M., Iedema, M., Yu, X.-Y., and Cowin, J. P.: Ionic strength dependence of the oxidation of SO<sub>2</sub> by H<sub>2</sub>O<sub>2</sub> in sodium chloride particles, *Atmospheric Environment*, 89, 731-738, 2014.
- Beltran, F. J.: *Ozone reaction kinetics for water and wastewater systems*, crc Press, 2003.
- 185 Burkholder, J., Sander, S., Abbatt, J., Barker, J., Cappa, C., Crounse, J., Dibble, T., Huie, R., Kolb, C., and Kurylo, M.: Chemical kinetics and photochemical data for use in atmospheric studies; evaluation number 19, Pasadena, CA: Jet Propulsion Laboratory, National Aeronautics and Space ..., 2020.
- Chang, Y., Huang, K., Deng, C., Zou, Z., Liu, S., and Zhang, Y.: First long-term and near real-time measurement of atmospheric trace elements in Shanghai, China, *Atmos. Chem. Phys. Discuss.*, in Review, 2017.
- 190 Cheng, Y., Zheng, G., Wei, C., Mu, Q., Zheng, B., Wang, Z., Gao, M., Zhang, Q., He, K., and Carmichael, G.: Reactive nitrogen chemistry in aerosol water as a source of sulfate during haze events in China, *Science Advances*, 2, e1601530, 2016a.
- Cheng, Y., Zheng, G., Wei, C., Mu, Q., Zheng, B., Wang, Z., Gao, M., Zhang, Q., He, K., Carmichael, G., Pöschl, U., and Su, H.: Reactive nitrogen chemistry in aerosol water as a source of sulfate during haze events in China, *Science Advances*, 2, e1601530, 10.1126/sciadv.1601530, 2016b.
- 195 Chung, M. Y., Muthana, S., Paluyo, R. N., and Hasson, A. S.: Measurements of effective Henry's law constants for hydrogen peroxide in concentrated salt solutions, *Atmospheric Environment*, 39, 2981-2989, 2005.
- Clegg, S., Kleeman, M., Griffin, R., and Seinfeld, J.: Effects of uncertainties in the thermodynamic properties of aerosol components in an air quality model—Part 1: Treatment of inorganic electrolytes and organic compounds in the condensed phase, *Atmospheric Chemistry and Physics*, 8, 1027-1085, 2008.
- 200 Clever, H. L.: Setchenov salt-effect parameter, *Journal of Chemical and Engineering Data*, 28, 340-343, 1983.
- Clifton, C. L., Altstein, N., and Huie, R. E.: Rate constant for the reaction of nitrogen dioxide with sulfur (IV) over the pH range 5.3-13, *Environmental science & technology*, 22, 586-589, 1988.
- Cui, Y., Ji, D., Chen, H., Gao, M., Maenhaut, W., He, J., and Wang, Y.: Characteristics and sources of hourly trace elements in airborne fine particles in urban Beijing, China, *Journal of Geophysical Research: Atmospheres*, 124, 11595-11613, 2019.
- 205 Cui, Y., Ji, D., He, J., Kong, S., and Wang, Y.: In situ continuous observation of hourly elements in PM<sub>2.5</sub> in urban Beijing, China: Occurrence levels, temporal variation, potential source regions and health risks, *Atmospheric Environment*, 222, 117164, 2020.
- Duan, J. C., Tan, J. H., Wang, S. L., Hao, J. M., and Chail, F. H.: Size distributions and sources of elements in particulate matter at curbside, urban and rural sites in Beijing, *Journal of Environmental Sciences*, 24, 87-94, 10.1016/s1001-0742(11)60731-6, 2012.
- 210 Fountoukis, C., and Nenes, A.: ISORROPIA II: a computationally efficient thermodynamic equilibrium model for K<sup>+</sup>-Ca<sup>2+</sup>-Mg<sup>2+</sup>-NH<sub>4</sub><sup>+</sup>-Na<sup>+</sup>-SO<sub>4</sub><sup>2-</sup>-NO<sub>3</sub><sup>-</sup>-Cl-H<sub>2</sub>O aerosols, *Atmospheric Chemistry and Physics*, 7, 4639-4659, 2007a.
- Fountoukis, C., and Nenes, A.: ISORROPIA II: a computationally efficient thermodynamic equilibrium model for K<sup>+</sup>-Ca<sup>2+</sup>-Mg<sup>2+</sup>-NH<sub>4</sub><sup>+</sup>-Na<sup>+</sup>-SO<sub>4</sub><sup>2-</sup>-NO<sub>3</sub><sup>-</sup>-Cl-H<sub>2</sub>O aerosols, *Atmospheric Chemistry and Physics Discussions*, 7, 1893-1939, 2007b.
- 215 Gao, J., Wang, K., Wang, Y., Liu, S., Zhu, C., Hao, J., Liu, H., Hua, S., and Tian, H.: Temporal-spatial characteristics and source apportionment of PM<sub>2.5</sub> as well as its associated chemical species in the Beijing-Tianjin-Hebei region of China, *Environmental Pollution*, 233, 714-724, 2018.
- Guo, H., Weber, R. J., and Nenes, A.: High levels of ammonia do not raise fine particle pH sufficiently to yield nitrogen oxide-dominated sulfate production, *Scientific Reports*, 7, 12109, 10.1038/s41598-017-11704-0, 2017.
- 220 He, R.-D., Zhang, Y.-S., Chen, Y.-Y., Jin, M.-J., Han, S.-J., Zhao, J.-S., Zhang, R.-Q., and Yan, Q.-S.: Heavy metal pollution characteristics and ecological and health risk assessment of atmospheric PM<sub>2.5</sub> in a living area of Zhengzhou City, *Huan jing ke xue= Huanjing kexue*, 40, 4774-4782, 2019.
- Herrmann, H., Schaefer, T., Tilgner, A., Styler, S. A., Weller, C., Teich, M., and Otto, T.: Tropospheric Aqueous-Phase Chemistry: Kinetics, Mechanisms, and Its Coupling to a Changing Gas Phase, *Chemical Reviews*, 115, 4259-4334, 10.1021/cr500447k, 2015.
- 225 Huss Jr, A., Lim, P. K., and Eckert, C.: Oxidation of aqueous sulfur dioxide. 1. Homogeneous manganese (II) and iron (II) catalysis at low pH, *The Journal of Physical Chemistry*, 86, 4224-4228, 1982.

- Ibusuki, T., and Takeuchi, K.: Sulfur dioxide oxidation by oxygen catalyzed by mixtures of manganese(II) and iron(III) in aqueous solutions at environmental reaction conditions, *Atmospheric Environment* (1967), 21, 1555-1560, [https://doi.org/10.1016/0004-6981\(87\)90317-9](https://doi.org/10.1016/0004-6981(87)90317-9), 1987.
- 230 Jain, S., Sharma, S., Vijayan, N., and Mandal, T.: Seasonal characteristics of aerosols (PM<sub>2.5</sub> and PM<sub>10</sub>) and their source apportionment using PMF: a four year study over Delhi, India, *Environmental Pollution*, 262, 114337, 2020.
- Kontogeorgis, G. M., Maribo-Mogensen, B., and Thomsen, K.: The Debye-Hückel theory and its importance in modeling electrolyte solutions, *Fluid Phase Equilibria*, 462, 130-152, 2018.
- 235 Kosak-Channing, L. F., and Helz, G. R.: Solubility of ozone in aqueous solutions of 0-0.6 M ionic strength at 5-30. degree. C, *Environmental science & technology*, 17, 145-149, 1983.
- Lagrange, J., Pallares, C., Wenger, G., and Lagrange, P.: Electrolyte effects on aqueous atmospheric oxidation of sulphur dioxide by hydrogen peroxide, *Atmospheric Environment. Part A. General Topics*, 27, 129-137, [https://doi.org/10.1016/0960-1686\(93\)90342-V](https://doi.org/10.1016/0960-1686(93)90342-V), 1993.
- 240 Lee, Y., and Schwartz, S. E.: Kinetics of oxidation of aqueous sulfur (IV) by nitrogen dioxide, *Precipitation Scavenging, Dry Deposition and Resuspension*, 1, 453-470, 1983.
- Li, J., Polka, H.-M., and Gmehling, J.: A gE model for single and mixed solvent electrolyte systems: 1. Model and results for strong electrolytes, *Fluid Phase Equilibria*, 94, 89-114, 1994.
- Linder, P. W., and Murray, K.: Correction of formation constants for ionic strength, from only one or two data points: An examination of the use of the extended Debye-Hückel equation, *Talanta*, 29, 377-382, 1982.
- 245 Liu, M., Song, Y., Zhou, T., Xu, Z., Yan, C., Zheng, M., Wu, Z., Hu, M., Wu, Y., and Zhu, T.: Fine particle pH during severe haze episodes in northern China, *Geophysical Research Letters*, 44, 5213-5221, <https://doi.org/10.1002/2017GL073210>, 2017.
- Liu, T., Clegg, S. L., and Abbatt, J. P. D.: Fast oxidation of sulfur dioxide by hydrogen peroxide in deliquesced aerosol particles, *Proceedings of the National Academy of Sciences*, 117, 1354-1359, 10.1073/pnas.1916401117, 2020.
- 250 Maahs, H. G.: Kinetics and mechanism of the oxidation of S(IV) by ozone in aqueous solution with particular reference to SO<sub>2</sub> conversion in nonurban tropospheric clouds, *Journal of Geophysical Research: Oceans*, 88, 10721-10732, <https://doi.org/10.1029/JC088iC15p10721>, 1983.
- Maaß, F., Elias, H., and Wannowius, K. J.: Kinetics of the oxidation of hydrogen sulfite by hydrogen peroxide in aqueous solution:: ionic strength effects and temperature dependence, *Atmospheric Environment*, 33, 4413-4419, 1999.
- 255 Martin, L. R., and Hill, M. W.: The iron catalyzed oxidation of sulfur: Reconciliation of the literature rates, *Atmospheric Environment* (1967), 21, 1487-1490, 1967.
- Martin, L. R., and Hill, M. W.: The effect of ionic strength on the manganese catalyzed oxidation of sulfur (IV), *Atmospheric Environment* (1967), 21, 2267-2270, 1987.
- McArdle, J. V., and Hoffmann, M. R.: Kinetics and mechanism of the oxidation of aquated sulfur dioxide by hydrogen peroxide at low pH, *The Journal of Physical Chemistry*, 87, 5425-5429, 1983.
- 260 Millero, F. J., Hershey, J. B., Johnson, G., and Zhang, J.-Z.: The solubility of SO<sub>2</sub> and the dissociation of H<sub>2</sub>SO<sub>3</sub> in NaCl solutions, *J Atmos Chem*, 8, 377-389, 1989.
- Ming, Y., and Russell, L. M.: Thermodynamic equilibrium of organic-electrolyte mixtures in aerosol particles, *AIChE Journal*, 48, 1331-1348, 2002.
- 265 Pitzer, K. S.: Ion interaction approach: theory and data correlation, *Activity coefficients in electrolyte solutions*, 2, 75-153, 1991.
- Polka, H.-M., Li, J., and Gmehling, J.: A gE model for single and mixed solvent electrolyte systems: 2. Results and comparison with other models, *Fluid phase equilibria*, 94, 115-127, 1994.
- Raatikainen, T., and Laaksonen, A.: Application of several activity coefficient models to water-organic-electrolyte aerosols of atmospheric interest, 2005.
- 270 Rischbieter, E., Stein, H., and Schumpe, A.: Ozone solubilities in water and aqueous salt solutions, *Journal of Chemical & Engineering Data*, 45, 338-340, 2000.
- Ross, H. B., and Noone, K. J.: A numerical investigation of the destruction of peroxy radical by Cu ion catalyzed-reactions of atmospheric particles, *J Atmos Chem*, 12, 121-136, 10.1007/bf00115775, 1991.
- 275 Rusumdar, A., Wolke, R., Tilgner, A., and Herrmann, H.: Treatment of non-ideality in the SPACCIM multiphase model-Part 1: Model development, 2016.

- Rusumdar, A. J., Tilgner, A., Wolke, R., and Herrmann, H.: Treatment of non-ideality in the SPACCIM multiphase model – Part 2: Impacts on the multiphase chemical processing in deliquesced aerosol particles, *Atmos. Chem. Phys.*, 20, 10351-10377, 10.5194/acp-20-10351-2020, 2020.
- 280 Seinfeld, J. H., and Pandis, S. N.: *Atmospheric chemistry and physics: from air pollution to climate change*, John Wiley & Sons, 2016.
- Sofowote, U. M., Di Federico, L. M., Healy, R. M., Debosz, J., Su, Y., Wang, J., and Munoz, A.: Heavy metals in the near-road environment: Results of semi-continuous monitoring of ambient particulate matter in the greater Toronto and Hamilton area, *Atmospheric Environment: X*, 1, 100005, 2019.
- 285 Wang, X., Gemayel, R., Hayeck, N., Perrier, S., Charbonnel, N., Xu, C., Chen, H., Zhu, C., Zhang, L., Wang, L., Nizkorodov, S. A., Wang, X., Wang, Z., Wang, T., Mellouki, A., Riva, M., Chen, J., and George, C.: Atmospheric Photosensitization: A New Pathway for Sulfate Formation, *Environmental Science & Technology*, 54, 3114-3120, 10.1021/acs.est.9b06347, 2020.
- Yu, Y., He, S., Wu, X., Zhang, C., Yao, Y., Liao, H., Wang, Q. g., and Xie, M.: PM<sub>2.5</sub> elements at an urban site in Yangtze River Delta, China: High time-resolved measurement and the application in source apportionment, *Environmental Pollution*, 253, 1089-1099, 2019.
- 290 Zhang, B., Zhou, T., Liu, Y., Yan, C., Li, X., Yu, J., Wang, S., Liu, B., and Zheng, M.: Comparison of water-soluble inorganic ions and trace metals in PM<sub>2.5</sub> between online and offline measurements in Beijing during winter, *Atmospheric Pollution Research*, 10, 1755-1765, <https://doi.org/10.1016/j.apr.2019.07.007>, 2019.
- Zhao, S., Tian, H., Luo, L., Liu, H., Wu, B., Liu, S., Bai, X., Liu, W., Liu, X., Wu, Y., Lin, S., Guo, Z., Lv, Y., and Xue, Y.: 295 Temporal variation characteristics and source apportionment of metal elements in PM<sub>2.5</sub> in urban Beijing during 2018–2019, *Environmental Pollution*, 268, 115856, <https://doi.org/10.1016/j.envpol.2020.115856>, 2021.
- Zheng, H., Song, S., Sarwar, G., Gen, M., Wang, S., Ding, D., Chang, X., Zhang, S., Xing, J., Sun, Y., Ji, D., Chan, C. K., Gao, J., and McElroy, M. B.: Contribution of Particulate Nitrate Photolysis to Heterogeneous Sulfate Formation for Winter Haze in China, *Environmental Science & Technology Letters*, 7, 632-638, 10.1021/acs.estlett.0c00368, 2020.
- 300 Zuend, A., Marcolli, C., Luo, B. P., and Peter, T.: A thermodynamic model of mixed organic-inorganic aerosols to predict activity coefficients, 2008.
- Zuend, A., Marcolli, C., Booth, A., Lienhard, D. M., Soonsin, V., Krieger, U., Topping, D. O., McFiggans, G., Peter, T., and Seinfeld, J. H.: New and extended parameterization of the thermodynamic model AIOMFAC: calculation of activity 305 coefficients for organic-inorganic mixtures containing carboxyl, hydroxyl, carbonyl, ether, ester, alkenyl, alkyl, and aromatic functional groups, *Atmospheric Chemistry and Physics*, 11, 9155-9206, 2011.